

# Adaptive Clutter Suppression and Detection Algorithm for Radar Maneuvering Target With High-Order Motions Via Sparse Fractional Ambiguity Function

Xiaolong Chen , Xiaohan Yu , Yong Huang, and Jian Guan

**Abstract**—Radar maneuvering target detection in clutter background should not only consider the complex characteristics of the target to accumulate its energy as much as possible, but also suppress clutter to improve the signal-to-clutter ratio (SCR). The traditional fractional domain transform-based detection method requires parameters match searching, which costs heavy computational burden in case of a large amount of data. Sparse FT and sparse fractional FT can obtain high-resolution sparse representation of the target, but the signal sparsity needs to be known before, and the sparse representation performance is poor in clutter background. In this article, adaptive filtering method is introduced into the sparse fractional ambiguity function (SFRAF) method, and a SFRAF domain adaptive clutter suppression and highly maneuvering target detection algorithm is proposed, which is named as adaptive SFRAF (ASFRAF). The ASFRAF domain iterative filtering operation can suppress the clutter while retaining the signal energy as much as possible. Simulation results and measured radar data processing results show that the proposed algorithm can overcome the limitation of the SFRAF on the sparsity preset value and achieve high efficiency and robust detection of high-order phase maneuvering targets under a low SCR environment.

**Index Terms**—Adaptive sparse fractional ambiguity function (ASFRAF), clutter suppression, least mean square (LMS) adaptive filter, radar maneuvering target detection, sparse representation.

## I. INTRODUCTION

THE rapid and effective detection of low observable maneuvering targets is a worldwide difficult problem in the field of radar technology [1]–[4]. Influenced by the complex environment (noise or clutter) and the complex motion characteristics of the target (acceleration, jerk, high-order motion, or

micromotion), the signal-to-clutter ratio (SCR) of the maneuvering target is low, and the echo Doppler exhibits time-varying characteristics. The acceleration caused by the speed change of the target, and the fluctuation of the marine target under high sea conditions would easily lead to high-order phase of the signal, which increases the difficulty of radar detection [5], [6]. With the development of novel radar systems such as phased array radar (PAR), ubiquitous radar [7], and multiple-input multiple-output (MIMO) radar [8], [9], the observation time of the target is greatly extended, which is beneficial to increase the integration gain and improve the refinement processing ability of maneuvering target in the clutter background [10]–[12]. However, this staring observation or the ubiquitous observation mode would increase the number of echo data, and the high system sampling frequency would further increase the amount of data, which puts higher requirements on the algorithm's calculation efficiency and system real-time performance [13].

In recent years, the development of sparse signal processing technology has provided new research ideas for radar target detection [14]–[17]. Since the moving target's signal has a certain sparse characteristic in a certain domain, the moving target detection problem can be converted into a sparse solution and the detection in the sparse domain. Then, high-resolution representation of the signal can be achieved in its corresponding sparse domain. At present, the moving target detection methods based on sparse representation can be divided into three kinds. First, from the perspective of mixed signal sparse decomposition and sparse domain feature differences, the micromotion target detection and feature extraction method based on morphological component analysis is proposed for different source signals [16]. Different dictionaries are used for sparse representation, and clutter and moving targets can be distinguished. The second and third kinds are the calculations from the perspective of sparse optimization [17] and down sampling fast FT (FFT) [18]–[22], respectively. By constructing sparse time-frequency transform domain, the high-resolution and low-complexity time-frequency representation of time-varying signals can be realized in the time-sparse domain. Both of the methods combine time-frequency distribution-based moving target detection and the advantage of sparse representation.

Manuscript received October 23, 2019; revised November 16, 2019 and March 9, 2020; accepted March 13, 2020. Date of publication April 17, 2020; date of current version April 27, 2020. This work was supported in part by the National Natural Science Foundation of China under Grant 61871391, Grant 61931021, Grant U1933135, and Grant 61871392, in part by the National Defense Science Foundation (2019-JCJQ-JJ-o58), and in part by the Key Research and Development Program of Shandong under Grant 2019GSF111004. (Corresponding author: Xiaolong Chen.)

Xiaolong Chen, Yong Huang, and Jian Guan are with the Radar Target Detection Research Group, Naval Aviation University, Yantai 264001, China (e-mail: cxlexl1209@163.com; huangyong\_2003@163.com; guanjian\_68@163.com).

Xiaohan Yu is with the Naval Research Academy, Beijing 100061, China (e-mail: yxhyxh0803@163.com).

Digital Object Identifier 10.1109/JSTARS.2020.2981046

Among the three kinds of methods, the first kind requires strict and precise moving target model, and the selection of the dictionary is the key point. The second kind has good adaptive performance, but the sparse optimization solving process is more complicated. The third methods combine the advantages of FFT and sparse representation, which is suitable for long-term sequence signal analysis. The most representative methods are the sparse FT (SFT) proposed by Massanyeh *et al.* of Massachusetts Institute of Technology [18], [19] and the sparse FRFT (SFRFT) proposed by Ran *et al.* [23]. For a spectrum sparse  $N$ -point large-size input signal, the SFT can reduce the computational complexity to  $O(K\log_2 N)$ , where  $K$  is the sparsity of the signal, i.e., the number of large-value coefficients in the frequency domain. The SFT method has been successfully applied in spectrum sensing, image detection, medical imaging, etc., however, it is based on FT and, therefore, can only deal with stationary signals, which is not suitable for radar maneuvering target detection [24], [25]. SFRFT has a good processing performance on linear frequency modulation signal, and can improve the analysis efficiency of sparse signals under large data conditions. However, due to the model mismatch with real signals, it is unsuitable for high maneuvering target signals with cubic phase information. Moreover, the reconstruction and detection performance of SFT and SFRFT are designed for noise background, the performances will be significantly degraded in case of strong clutter backgrounds. Therefore, the detection performance is still difficult to meet the actual requirements.

The radar target detection research group from Naval Aviation University proposed several SFT-based moving target detection methods, i.e., adaptive dual-threshold sparse Fourier transform (ADT-SFT) [26] and robust SFRFT (RSFRFT) [27], which are more suitable for moving target detection in the clutter background. For highly maneuvering target detection, sparse fractional ambiguity function (SFRAF) [28] can not only achieve good aggregation of high-order phase signals by FRAF, but also achieve effective improvement of computational efficiency, and can realize rapid extraction of maneuvering targets under large data conditions. However, SFRAF has the following two defects when it is applied to the detection of maneuvering targets in the clutter background. On the one hand, SFRAF needs to preset the sparsity  $K$  of the signal, but in practical applications, the sparsity of the signal is often unknown or it may change (for example, the number of maneuvering targets or spectrum peaks), which reduces the robustness of the algorithm. On the other hand, SFRAF itself has no clutter suppression capability, and in the case of low SCR, the signal reconstruction reliability is poor.

Least mean square (LMS) adaptive filter [29]–[31] uses recursive algorithm for internal operations, which can overcome the limitation of prior information. It has the advantages of good robustness, simple structure, and small computational complexity. It is a powerful tool for signal filtering. However, the time-domain LMS adaptive algorithm is sensitive to the dispersion of the eigenvalues of the signal autocorrelation matrix, while the dispersion of the eigenvalues of the nonstationary signal autocorrelation matrix is large, and it would lead to the degradation of the convergence performance of the algorithm and poor filtering performance. Later, the input signal can be orthogonally

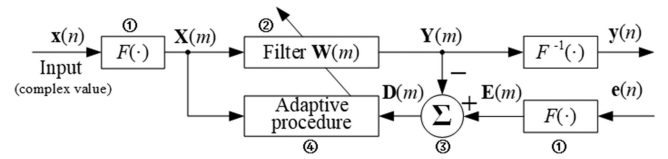


Fig. 1. Block diagram of transform domain adaptive filtering method.

transformed to filter in the transform domain to reduce the dispersion of the eigenvalues of the autocorrelation matrix, thereby improving the performance of the filtering algorithm. Transform domain adaptive filtering method, e.g., cosine transform domain LMS algorithm [32], wavelet transform domain LMS algorithm [33], [34], FRFT domain LMS algorithm [35], can improve the convergence of nonstationary signals, reduce steady-state error, and have good application prospects in spectrum line enhancement and clutter cancellation.

In this article, the adaptive filtering method is introduced into the SFRAF processing, and an adaptive clutter suppression and radar maneuvering target detection algorithm based on SFRAF is proposed, which is named as an adaptive SFRAF (ASFRAF). It not only takes the advantage of SFRAF in terms of high resolution and computational efficiency, but also realizes highly maneuvering target detection in a clutter background. First, the principle of transform domain adaptive filtering algorithm is introduced in Section II. Then, the SFRAF domain adaptive filtering algorithm is analyzed in detail in Section III. In Section IV, the adaptive clutter suppression and maneuvering target detection procedures of ASFRAF are given and the convergence performance of different parameters is studied. The simulations and the real radar experimental results show that the proposed method can suppress the clutter better while retaining the signal energy to the greatest extent, and still has good detection performance for the maneuvering target in the case of low SCR. The detection performance and complexity of the proposed algorithm are analyzed as well in Section V. Section VI concludes the article and presents its future research directions.

## II. PRINCIPLE OF TRANSFORM DOMAIN ADAPTIVE FILTERING ALGORITHM

Fig. 1 shows the block diagram of the transform domain adaptive filtering method. In the figure,  $\mathbf{x}(n)$  is an  $N$ -dimensional input complex signal vector,  $\mathbf{e}(n)$  is an  $N$ -dimensional expected signal vector,  $F(\cdot)$  represents transformation, and  $\mathbf{X}(m)$  and  $\mathbf{E}(m)$  are the transforms of  $\mathbf{x}(n)$  and  $\mathbf{e}(n)$ , respectively.  $\mathbf{W}(m)$  is the filter weight coefficient vector,  $F^{-1}(\cdot)$  represents the inverse transform, and  $\mathbf{y}(n)$  is the output signal vector. The arrow in the figure stands for filtering symbol. The transform domain adaptive filtering mainly consists of four steps.

- 1) Perform  $F(\cdot)$  transformation on the input signal  $\mathbf{x}(n)$  and expected signal  $\mathbf{e}(n)$  to get the transform results  $\mathbf{X}(m)$  and  $\mathbf{E}(m)$ , respectively.
- 2) Obtain the transform domain output signal  $\mathbf{Y}(m)$  by using the filter weight coefficient vector  $\mathbf{W}(m)$ , namely

$$\mathbf{Y}(m) = \mathbf{X}_{\text{dia}}(m)\mathbf{W}(m) \quad (1)$$

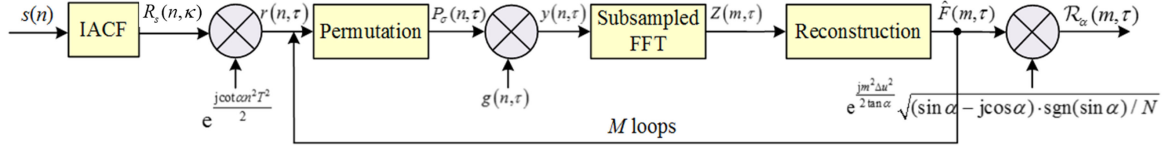


Fig. 2. Flowchart of the SFRAF.

where  $\mathbf{X}_{\text{dia}}(m)$  represents a  $N \times N$ -dimensional diagonal matrix corresponding to  $\mathbf{X}(m)$ .

- 3) Calculate the error vector  $\mathbf{D}(m)$  as following:

$$\mathbf{D}(m) = \mathbf{E}(m) - \mathbf{Y}(m). \quad (2)$$

- 4) Adaptive procedure. Update the weight coefficient vector of the filter automatically according to the recursive formula to achieve adaptive iteration until the steady state is reached

$$\mathbf{W}(m+1) = \mathbf{W}(m) + \mu \mathbf{X}_{\text{dia}}^H(m) \mathbf{D}(m) \quad (3)$$

where  $\mu$  is the adaptive step size.

### III. SFRAF DOMAIN ADAPTIVE FILTERING ALGORITHM

#### A. Principle of SFRAF

The detailed procedure of the SFRAF is shown in Fig. 2. For a maneuvering target in clutter background modeled as quadratic frequency modulated (QFM) signal [6], the discrete signal can be expressed as

$$x(n\Delta t) = A_0 \exp [j2\pi (a_0 + a_1 n\Delta t + a_2 n^2 \Delta t^2 + a_3 n^3 \Delta t^3)] + c(n\Delta t), \quad n \in [1, N] \quad (4)$$

where  $A_0$  is the signal amplitude,  $a_i (i = 0, 1, 2, 3)$  is the polynomial coefficients, i.e.,  $a_0 = 2R_0/\lambda$ ,  $a_1 = 2v_0/\lambda$ ,  $a_2 = a_s/\lambda$ ,  $a_3 = g_s/3\lambda$ ,  $R_0$  is the initial distance,  $v_0$ ,  $a_s$ ,  $g_s$  represent initial velocity, acceleration, and jerk respectively,  $\lambda$  is the wavelength,  $\Delta t = 1/f_s$  is the sampling interval,  $N = T_n \cdot f_s$  is the sampling number, the observation time  $T_n$ , and the sampling frequency  $f_s$ ,  $c(n\Delta t)$  is the clutter.

The SFRAF  $\mathcal{R}_\alpha()$  with transform angle  $\alpha$  is defined as follows:

$$\mathcal{R}_\alpha(m, \tau) = \mathcal{C}_m \left( \mathcal{S} \left[ \mathcal{C}_n \left( \underbrace{R_s(n, \kappa)}_{\text{IACF}} \right) \right] \right) \quad (5)$$

where  $m \in [1, N]$  is the discrete variable in SFRAF domain,  $\mathcal{C}()$  and  $\mathcal{S}()$  represent the chirp and SFT operators, respectively.  $R_s()$  is the IACF calculation

$$\begin{aligned} R_s(n, \tau) &= x(n\Delta t + \kappa/2) x^*(n\Delta t - \kappa/2) \\ &= A_0^2 \exp [j2\pi \kappa (a_1 + 2a_2 n\Delta t + 3a_3 n^2 \Delta t^2 \\ &\quad + a_3 \kappa^2/4)] + R_c(n, \kappa) + R_{sc}(n, \kappa) \end{aligned} \quad (6)$$

where  $\kappa$  is a time delay,  $R_c(n, \kappa)$  and  $R_{sc}(n, \kappa)$  are the IACFs of autoterm of clutter and cross terms between clutter and target.

After the IACF, the remaining procedure of SFRAF is the same as the SFRFT [23], which is composed of five parts, i.e.,

chirp1 multiplication, spectrum permutation, window function filtering, subsampled-FFT, reconstruction, and chirp2 multiplication. Normally, the time delay is a constant value [6]. Supposing the spectrum after reconstruction is  $\hat{F}(m)$ , the final result of SFRAF is  $\mathcal{R}_\alpha(m)$ .

#### B. Principle of SFRAF Adaptive Filtering (ASFRAF)

SFRAF has good energy aggregation for QFM signals. In a particular SFRAF domain, the target signal can be regarded as a narrowband signal, and the clutter is a wideband signal. Therefore, by setting a suitable delay  $\tau$  for the signal  $x(n)$ , the clutter is decorrelated, which is helpful for clutter suppression and target enhancement. For radar, the input signal  $x(n)$  represents the radar returns after demodulation and pulse compression, which is complex composed with  $I$  and  $Q$  two channels.

The delayed signal is used as the expected signal  $e(n)$ , and the input complex vector  $\mathbf{x}(n)$  and  $\mathbf{e}(n)$  are subjected to SFRAF operation, respectively, with the processing results  $\mathbf{X}_p(m)$  are  $\mathbf{E}_p(m)$ , where  $p$  is the transform order. Then, the output of the filter is

$$\mathbf{Y}_p(m) = \mathbf{X}_{\text{dia}}(m) \mathbf{W}(m) \quad (7)$$

where  $\mathbf{X}_{\text{dia}}(m)$  represents a diagonal  $N \times N$  matrix corresponding to  $\mathbf{X}_p(m)$ , and the corresponding error vector is

$$\mathbf{D}_p(m) = \mathbf{E}_p(m) - \mathbf{Y}_p(m). \quad (8)$$

The iterative formula (3) has a strong memory effect on the initial frequency of the signal. Under strong clutter interference, the tracking performance of the filter is susceptible to residual clutter. By setting the time-varying weight coefficient vector and performing power normalization on the adaptive step size, the tracking performance of the filter in the clutter environment can be improved as well as the convergence speed of the filter [35]. At this time, the update formula of the weight coefficient vector is

$$\mathbf{W}(m+1) = \mathbf{H}(z) \mathbf{W}(m) + \mu_{\text{NLMS}} \mathbf{X}_{\text{dia}}^H(m) \mathbf{D}_p(m) \quad (9)$$

where  $\mathbf{H}(z)$  is the leak response function. When  $\mathbf{H}(z) = \chi \mathbf{I}$  ( $\mathbf{I}$  is a unit matrix), the above equation can be converted into

$$\mathbf{W}(m+1) = \chi \mathbf{W}(m) + \mu_{\text{NLMS}} \mathbf{X}_{\text{dia}}^H(m) \mathbf{D}_p(m) \quad (10)$$

where  $\chi$  is the leakage factor and  $\mu_{\text{NLMS}}$  is the normalized adaptive step size expressed as follows:

$$\mu_{\text{NLMS}} = \frac{\mu}{\xi + \mathbf{X}_p^H(m) \mathbf{X}_p(m)} \quad (11)$$

where  $\xi$  is a positive constant value.

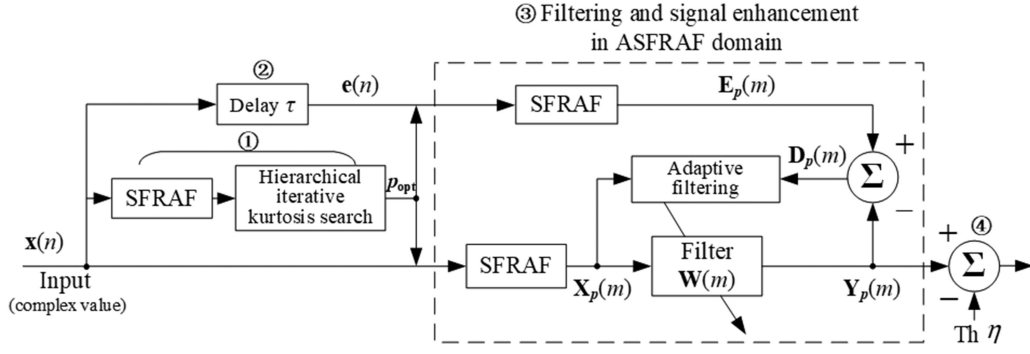


Fig. 3. Clutter suppression and maneuvering target detection method based on ASFRAF.

TABLE I  
IMPLEMENTATION PSEUDOCODE OF THE ASFRAF ALGORITHM

<b>Input</b> $x(n)$
<b>Output</b> $Y_p(m)$
<b>Initial condition</b> $W(0)=0$
1. Data selection: $\mathbf{x}(n) \leftarrow x(n)$
2. Optimal transform order calculation: $p_{opt} \leftarrow p$
3. <b>for</b> $l = 1 : L$ ( $L$ is the iteration times)
4. Time delay: $\mathbf{e}(n) \leftarrow \mathbf{x}(n), \tau$
5. SFRAF calculation: $\mathbf{X}_p(m) \leftarrow \mathbf{x}(n), \mathbf{E}_p(m) \leftarrow \mathbf{e}(n)$
6. Filtering: $\mathbf{Y}_p(m) \leftarrow \mathbf{X}_{dia}(m)$
7. Estimation error: $\mathbf{D}_p(m) \leftarrow \mathbf{Y}_p(m)$
8. Weight vector coefficient update: $\mathbf{W}(m+1) \leftarrow \mathbf{D}_p(m)$
9. <b>end for</b>
10. <b>return</b> $Y_p(m)$

The mean square error (MSE) of the filter can be defined as the mean square value of the error vector, namely

$$\delta(m) = \frac{E[\mathbf{D}_p^H(m)\mathbf{D}_p(m)]}{N} \quad (12)$$

where  $E[\ ]$  represents the expectation. According to [28], if the adaptive process of the algorithm converges, the condition should be

$$0 < \mu < 1 + \chi. \quad (13)$$

### C. Algorithm Flowchart

Table I shows the implementation pseudocode of the ASFRAF algorithm.

## IV. DETECTION OF MANEUVERING TARGET VIA ASFRAF

The detailed adaptive clutter suppression and maneuvering target detection process based on ASFRAF are shown in Fig. 3, which is composed of four main procedures.

1) Perform SFRAF processing on the input radar echo signal  $\mathbf{x}(n)$ , and quickly determine the optimal transform order  $p_{opt}$  by hierarchical iterative kurtosis search.

The traditional peak search method only uses the energy concentration of the QFM signal in the FRAF domain to suppress the clutter. Under the low SCR condition, the detection performance

will be seriously degraded, and when a higher parameter estimation accuracy is required, a small search step size is needed, which would increase the calculation burden greatly. It is found in [6] that when the QFM signal matches the rotation angle, its signal component will appear as a super-Gaussian signal in the fractional domain, and when the signal does not match the rotation angle, it will still appear as a QFM signal. Therefore, the kurtosis curve of the echo signal in the FRAF domain will have a peak point at the best transform order  $p_{opt}$ . The kurtosis of the input vector  $\mathbf{x}(n)$  is defined as [29]

$$K_x(i) = \frac{E[\mathbf{X}_{p_i}^4(m)]}{E^2[\mathbf{X}_{p_i}^2(m)]} - 2 \quad (14)$$

where  $\mathbf{X}_{p_i}(m)$  is the  $p_i$ -order SFRAF of  $\mathbf{x}(n)$ .

In order to reduce the amount of computation, a hierarchical iterative kurtosis search can be used to determine the optimal transform order. First, the search range of the transform order  $p$  is initially determined according to the radar parameters and the target motion state. Assuming that the initial search interval of  $p$  is  $[a_1, b_1]$ , the search step size  $l$  takes an order of magnitude lower than the length of the search interval. For example,  $\Delta_1 = b_1 - a_1 = 0.3 = 3 \times 10^{-1}$ , the initial search step size  $l_1 = 10^{-2}$ . Assume that the maximum kurtosis value obtained after the first search corresponds to the order of  $p_1$ , taking  $p_1$  as the initial value, and perform the hierarchical iteration according to the following formula:

$$\begin{cases} a_{j+1} = p_j - l_j \\ b_{j+1} = p_j + l_j \\ l_{j+1} = 0.1l_j \end{cases} \quad (15)$$

where  $[a_{j+1}, b_{j+1}]$  and  $l_{j+1}$  are the search interval and search step size for the  $j + 1$ th search, respectively,  $p_j$  is the best transform order for the  $j$ th search.  $p_j$  will approach the required accuracy in the form of an exponential power of 0.1.

Carry out the iteration calculation sequentially until  $l_j \leq \varepsilon$ , where  $\varepsilon$  is the estimation accuracy for the parameters. The hierarchical iterative kurtosis search can improve the computational efficiency of the algorithm, and the higher the accuracy of the required parameter estimation, the more obvious the improvement of the computational efficiency.

2) The  $\mathbf{x}(n)$  delay  $\tau$  is obtained to obtain the desired signal  $\mathbf{e}(n)$ .

TABLE II  
SIMULATION PARAMETERS

Parameters	Wavelength $\lambda$ (m)	Sampling number $N$	Sea state	Sampling frequency $f_s$ (Hz)
Value	0.033	8192	3	5000
Motion parameters	Initial velocity $v_0$ (m/s)	Acceleration $a_s$ (m/s <sup>2</sup> )	Jerk $g_s$ (m/s <sup>3</sup> )	
Value	1.667	8.333	6.667	

- 3) The ASFRAF domain adaptive operation is performed according to the algorithm description in Table I. When the error of the filter reaches steady state, the output result is  $\mathbf{Y}_p(m)$ .
- 4) Compare the ASFRAF amplitude of the output signal as the detection statistic with the threshold, and output the final detection result

$$|\mathbf{Y}_p(m)| \begin{cases} > \eta & H_1 \\ < \eta & H_0 \end{cases} \quad (16)$$

where  $\eta$  is detection threshold, which is determined by  $P_{fa}$ . If the detection statistic is lower than the detection threshold, it indicates that the rangebin has no maneuvering target. If the detection statistic is higher than the detection threshold, it indicates that the rangebin has the maneuvering target.

## V. EXPERIMENTAL RESULTS AND ANALYSIS

In this section, real radar data collected by the council for scientific and industrial research (CSIR) [36] are used to verify the performance of the proposed algorithm in sea clutter background. On the one hand, in order to explain the detail performance, pure sea clutter and simulated signals of maneuvering target are generated; on the other hand, real data of maneuvering target are used for the detection in complex time-varying environment. Moreover, the detection performance is compared with some traditional coherent integration methods, e.g., MTD, FRFT, and FRAF, as well as some sparse representation methods, e.g., SFT, SFRFT, SFRAF, and robust SFRFT (SFRFT). The computational time is calculated as well.

### A. Radar Data Analysis

The proposed algorithm is verified by the TFC17-006 data in the CSIR database. The radar and experimental parameters of the data are shown in Table II, and the time distance analysis and time-frequency analysis of the data are shown in Fig. 4. As can be seen from the figure, the 30th distance unit is a pure sea clutter rangebin, which is selected as the background. Supposing there is a maneuvering target with a center frequency  $a_1 = 100$  Hz, a modulation frequency  $a_2 = 500$  Hz/s, a secondary frequency  $a_3 = 400$  Hz/s<sup>2</sup>, the amplitude obeys the Rayleigh distribution, the simulation satisfies the sampling theorem, and the radar operating frequency is 9 GHz. The specific motion parameters are shown in Table II.

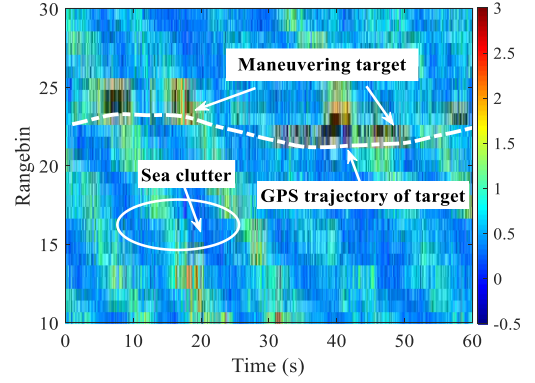


Fig. 4. Range versus time plot of TFC17-006.

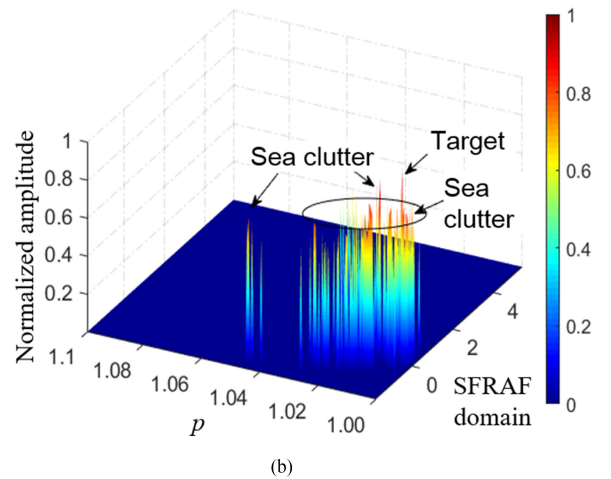
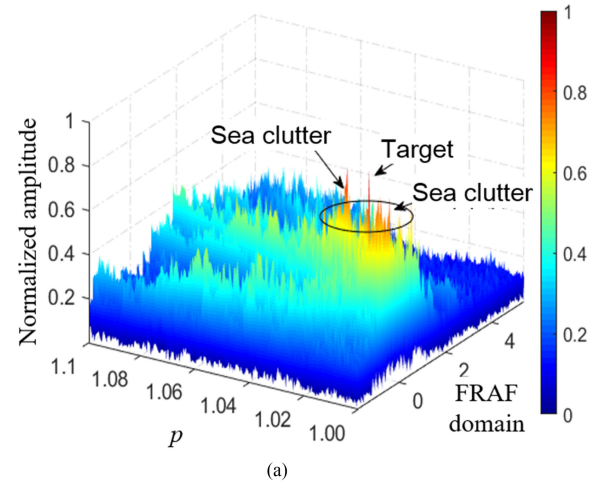


Fig. 5. FRAF and SFRAF of the radar returns (SCR = -5 dB). (a) FRAF. (b) SFRAF.

Fig. 5 shows the FRAF result of the generated signal when SCR = -5 dB. As can be seen from Fig. 5(a), FRAF has good energy concentration on the QFM signal, and the maneuvering target appears as a peak point in the FRAF domain. However, some components of sea clutter are also accumulated in the FRAF domain, which makes the target submerged in the clutter, causing great difficulties in detection. In addition, the SFT-based

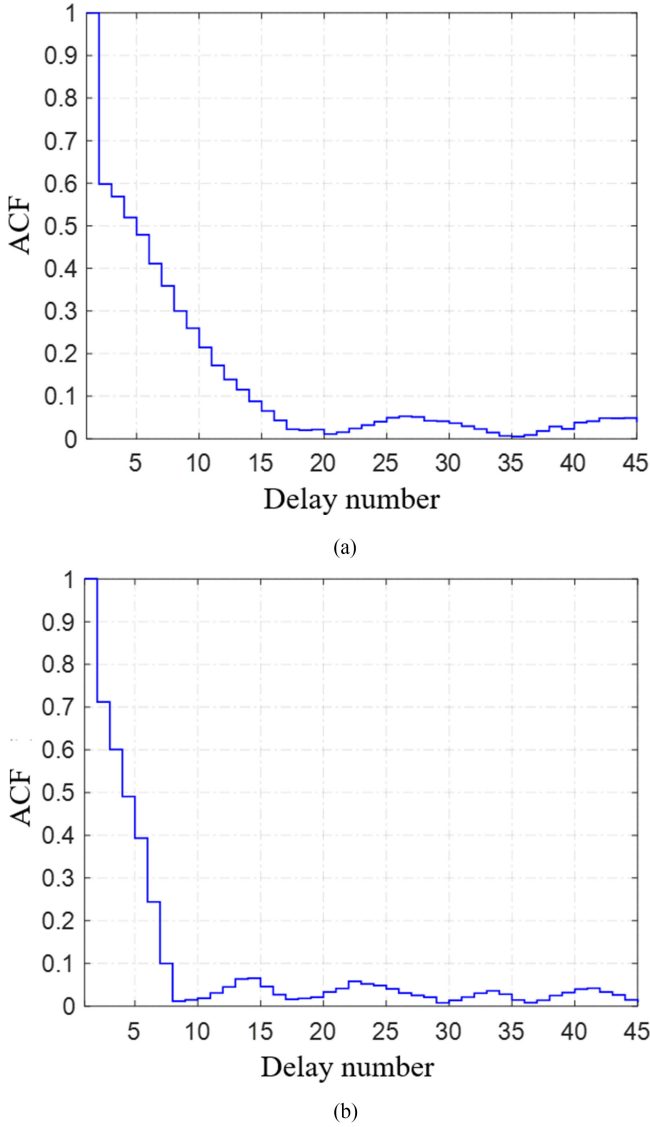


Fig. 6. ACF of radar returns in FRAF domain. (a) ACF of sea clutter (b) ACF of maneuvering target.

SFRAF has no clutter suppression capability, and the detection performance is seriously degraded under strong clutter interference, which is shown in Fig. 5(b). Therefore, it is necessary to improve the clutter suppression ability of SFRAF.

Assuming the parameter estimation accuracy  $\varepsilon = 10^{-4}$ , the initial search interval of the transform order  $p$  is  $[a_1, b_1] = [1, 1.2]$ , then the initial search step size  $l_1 = 10^{-2}$ . The optimal transform order is obtained by hierarchical iterative kurtosis search as  $p_{opt} = 1.0066$ . The number of times that the hierarchical iterative kurtosis search and the traditional peak search are  $M_1 = 60$  and  $M_1 = 2000$ , respectively. Therefore, the hierarchical iterative kurtosis search can greatly improve the computational efficiency.

### B. Parameters Selection

The problem of maneuvering target detection in clutter background can be regarded as the detection problem of narrowband

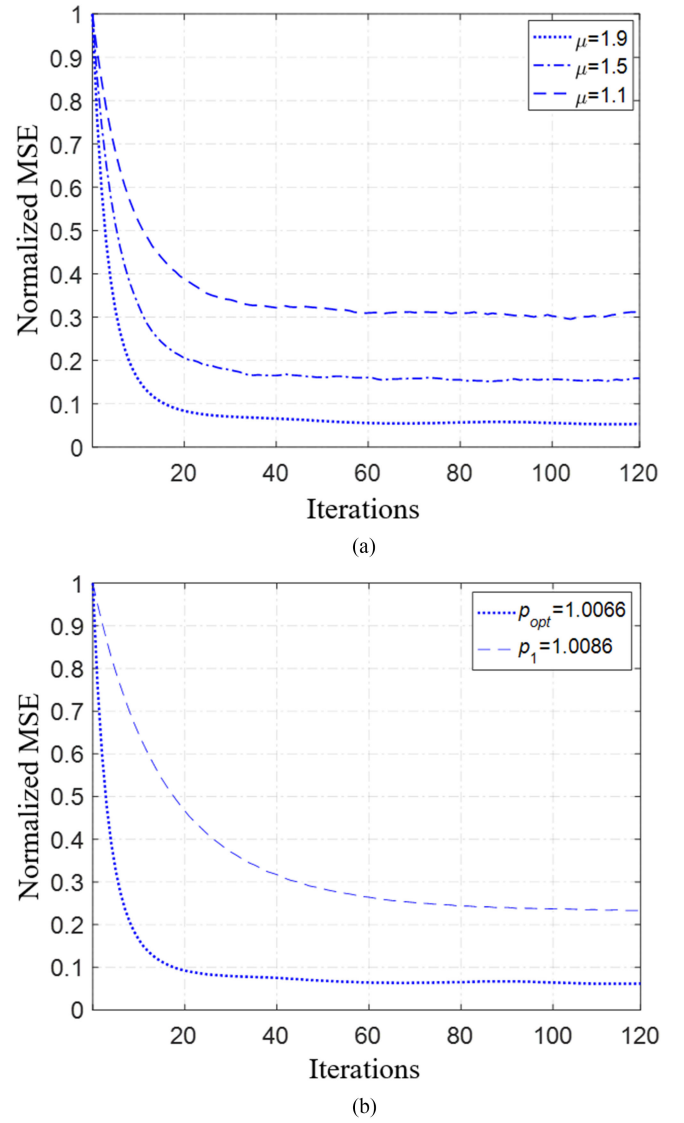


Fig. 7. Influence of different parameters on convergence performance of SFRAF domain adaptive line enhancer. (a) Different step sizes ( $\tau = 2$  ms,  $\chi = 0.97$ ,  $p = 1.0066$ ). (b) Different transform orders ( $\tau = 2$  ms,  $\chi = 0.97$ ,  $\mu = 1.9$ ).

signals in wideband signals. The correlation radius of the wideband signal should be greater than the correlation radius of the narrowband signal. Using this property, when the selected time delay  $\tau$  is longer than the correlation time of the target's signal and less than the correlation time of the clutter signal, the SFRAF domain adaptive algorithm can be used for the decorrelation of clutter. Then, the clutter suppression and target enhancement can be achieved. The correlation of the signal in the SFRAF domain can be measured by the autocorrelation function (ACF), which is defined as [35]

$$\text{ACF}_m = \frac{\sum_{i=1}^{N-1} X_p(i)X_p^*(i+m)}{\sum_{i=1}^{N-1} X_p(i)X_p^*(i)} \quad (17)$$

where  $m$  is the number of sampling points in the interval. The ACF represents the correlation time of  $m$  adjacent samples.

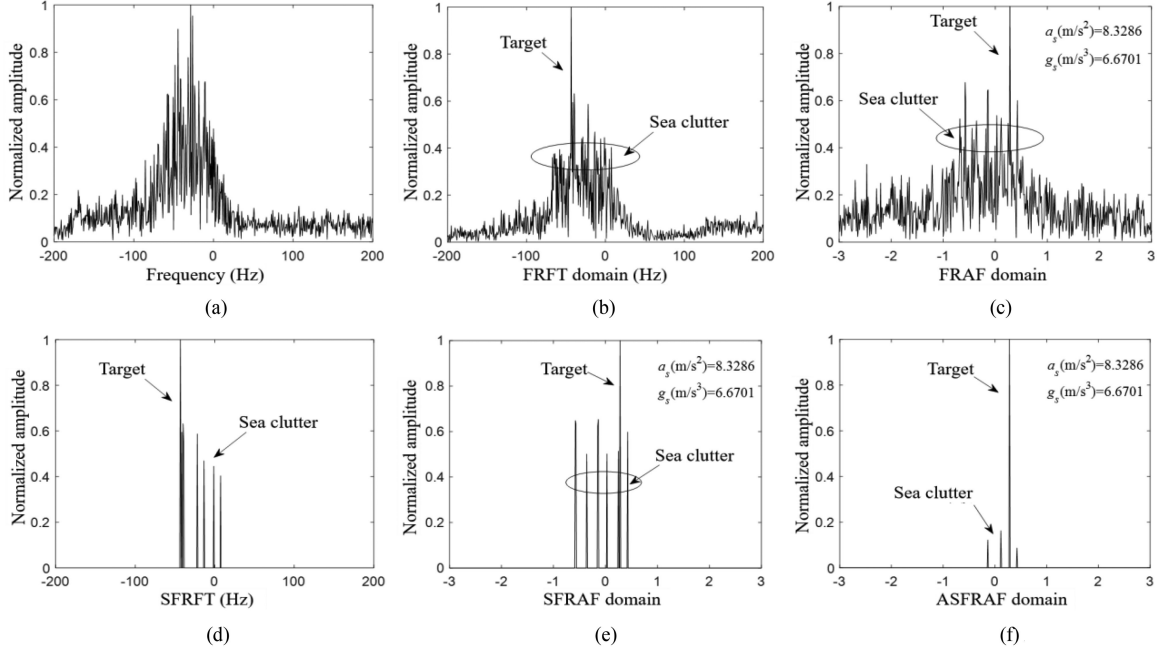


Fig. 8. Maneuvering target detection using different methods (SCR = -5 dB). (a) MTD. (b) FRFT ( $p_{\text{opt}} = 1.005$ ). (c) FRAF ( $p_{\text{opt}} = 1.0066$ ). (d) SFRFT ( $p_{\text{opt}} = 1.005$ ,  $K = 7$ ). (e) SFRAF ( $p_{\text{opt}} = 1.0066$ ,  $K = 7$ ). (f) ASFRAF ( $p_{\text{opt}} = 1.0066$ ,  $K = 7$ ).

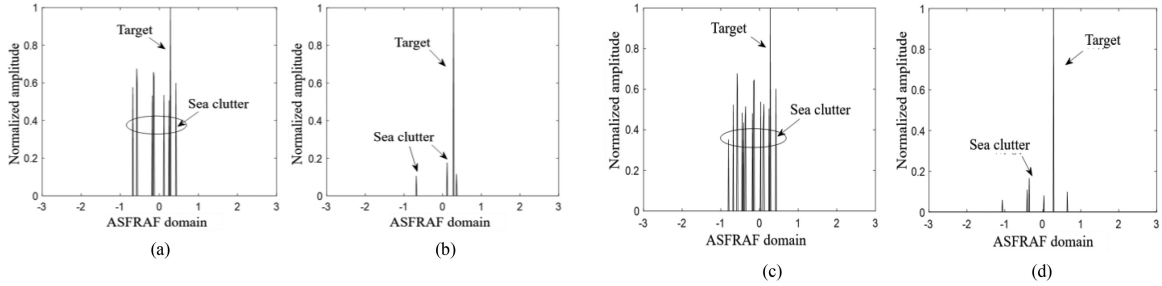


Fig. 9. Detection results comparisons of SFRAF and ASFRAF with different sparsity  $K$  (SCR = -5 dB,  $p_{\text{opt}} = 1.0066$ ). (a) SFRAF ( $K = 10$ ). (b) ASFRAF ( $K = 10$ ). (c) SFRAF ( $K = 15$ ). (d) ASFRAF ( $K = 15$ ).

Fig. 6 shows the ACF curves of the sea clutter and the target in the FRAF domain. It can be found that the correlation radius of the sea clutter in the FRAF domain is about 20 sampling points, and according to  $f_s = 5000$  Hz, the time delay is about 4 ms; while the correlation radius of the maneuvering target in the FRAF domain is only seven sampling points, and the corresponding time delay is 1.4 ms. Therefore, the signal of maneuvering target in the FRAF domain has a shorter correlation time than that of the sea clutter. The time delay of the SFRAF domain adaptive line enhancer should be in the range of  $1.4 \text{ ms} < \tau < 4 \text{ ms}$ .

In practical applications, in order to ensure the stability of the filter, the value of the leakage factor  $\chi$  is generally  $0.95 < \chi < 1$  [37]. In this section, it is set to  $\chi = 0.97$ , and the range of the adaptive step size is  $0 < \mu < 1.97$  obtained by (13). Taking  $\tau = 2$  ms,  $\xi \approx 0$ , and the sparsity  $K = 8$ , the effects of adaptive step size and transform order on the convergence performance of SFRAF domain adaptive filter are studied. Fig. 7 shows the relationships between different adaptive step sizes and transform orders as well as MSE in case of SCR = 3 dB. The  $x$ -axis is the number of

iterations of the filter, and the  $y$ -axis is the average MSE under 50 independent simulations, which is also normalized. Fig. 7(a) shows the relationship between different adaptive step sizes and MSE when  $p = 1.0066$ . The step values are  $\mu_1 = 1.9$ ,  $\mu_2 = 1.5$ , and  $\mu_3 = 1.1$ . As can be seen from the figure, the larger the step size, the smaller the MSE of the filter, and the faster speed of the convergence, the more stable the algorithm. Fig. 7(b) shows the relationship between different transform orders and MSE, with the step size  $\mu = 1.9$ . It can be found that the MSE of the filter can converge to the minimum value only when  $p = p_{\text{opt}}$ . However, when  $p$  takes other values, the convergence performance is worse because the transform angle does not match the target signal.

### C. Detection Results

Fig. 8 shows the detection results of FFT, FRFT, SFRFT, FRAF, SFRAF, and ASFRAF of CSIR data with SCR = -5 dB. Among them, FRFT and FRAF use the traditional peak search, the sparsity setting of the SFRFT and SFRAF algorithms is  $K = 7$ , the number of baskets is  $B = 256$ , the parameters of ASFRAF

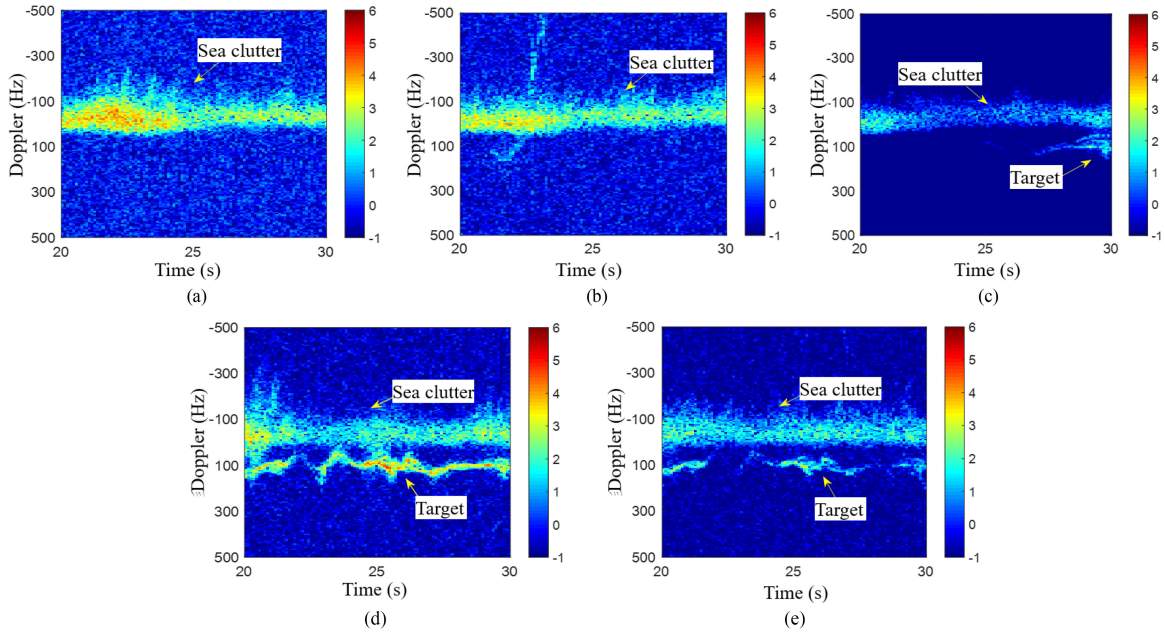


Fig. 10. Time-frequency plot of different rangebins (TFC17-006, 20 s–30 s). (a) Rangebin 21. (b) Rangebin 22. (c) Rangebin 23. (d) Rangebin 24. (e) Rangebin 25.

are  $\tau = 2$  ms,  $\chi = 0.97$ , and  $\mu = 1.9$ . Several results can be obtained:

- 1) Due to the obvious maneuverability of the target, it is difficult to find the target in the frequency domain.
- 2) The energy aggregation results of FRFT and SFRFT are better than the FFT, but the target cannot be effectively detected due to the transform model mismatched with the real signal.
- 3) FRAF and SFRAF can both accumulate the target's energy and detect the target better. Moreover, the computational complexity analysis in [28] shows that the SFRAF algorithm can greatly improve the computational efficiency. However, since the preset sparsity value of SFRAF may be inconsistent with the number of strong spectrum points of target, sea clutter will also be detected resulting in false alarms [see Fig. 8(e)], which will seriously affect the detection performance.
- 4) For the proposed ASFRAF algorithm, the sea clutter is suppressed greatly and at the same target's energy is remained. And there are almost no false alarms (sea clutter) remaining in the detection result [see Fig. 8(f)]. Although the preset sparsity value is inconsistent with the exact number, the detection result is less disturbed by the clutter, which shows the robustness of the algorithm. Therefore, the proposed ASFRAF domain adaptive detection method can effectively improve the maneuvering target detection performance in case of strong clutter environment.

The influence of different values of the sparsity  $K$  on the detection result of the ASFRAF algorithm is further studied. Fig. 9(a) and (b) shows the SFRAF and ASFRAF detection results with  $K = 10$ , and Fig. 9(c) and (b) correspond to the results for  $K = 15$ . Comparing Fig. 8(e)–(f) with Fig. 9, we can find that: 1) Although the value of sparsity is inconsistent with the real value,

TABLE III  
RESULTS COMPARISON OF DIFFERENT METHODS

	Target peak	Sea clutter peak	Peak difference	Time <sup>*</sup> (s)
FFT	1	0.9541	0.0459	0.0469
FRFT	1	0.6318	0.3682	1.8209
SFRFT ( $K=7$ )	1	0.6318	0.3682	0.0415
FRAF	1	0.6776	0.3224	2.3547
SFRAF ( $K=7$ )	1	0.6538	0.3462	0.0664
<b>ASFRAF (<math>K=7</math>)</b>	<b>1</b>	<b>0.1626</b>	<b>0.8374</b>	<b>0.9389</b>
SFRAF ( $K=10$ )	1	0.6754	0.3246	0.0792
<b>ASFRAF (<math>K=10</math>)</b>	<b>1</b>	<b>0.1763</b>	<b>0.8237</b>	<b>1.1578</b>
SFRAF ( $K=15$ )	1	0.6776	0.3224	0.0904
<b>ASFRAF (<math>K=15</math>)</b>	<b>1</b>	<b>0.1658</b>	<b>0.8342</b>	<b>1.5303</b>

\* Computer configuration: Intel Core i7-4790 3.6 GHz CPU; 16G RAM.

the clutter can be well suppressed in the ASFRAF domain, which indicates that the ASFRAF is less influenced by clutter. 2) Under the condition of different  $K$  values, although the number and amplitude of sea clutter in the ASFRAF domain are slightly different, the SCR as well as the clutter suppression capability are significantly improved compared with SFRAF. Therefore, we can draw the conclusion that the ASFRAF domain detection method can overcome the influence of the unknown sparsity value and enhance the robustness of the SFRAF algorithm.

Table III further quantitatively compares the detection results of the different methods in Figs. 8 and 9, and gives the specific target and sea clutter peak differences as well as the calculation time. The target's peak is normalized to 1 for better comparison.

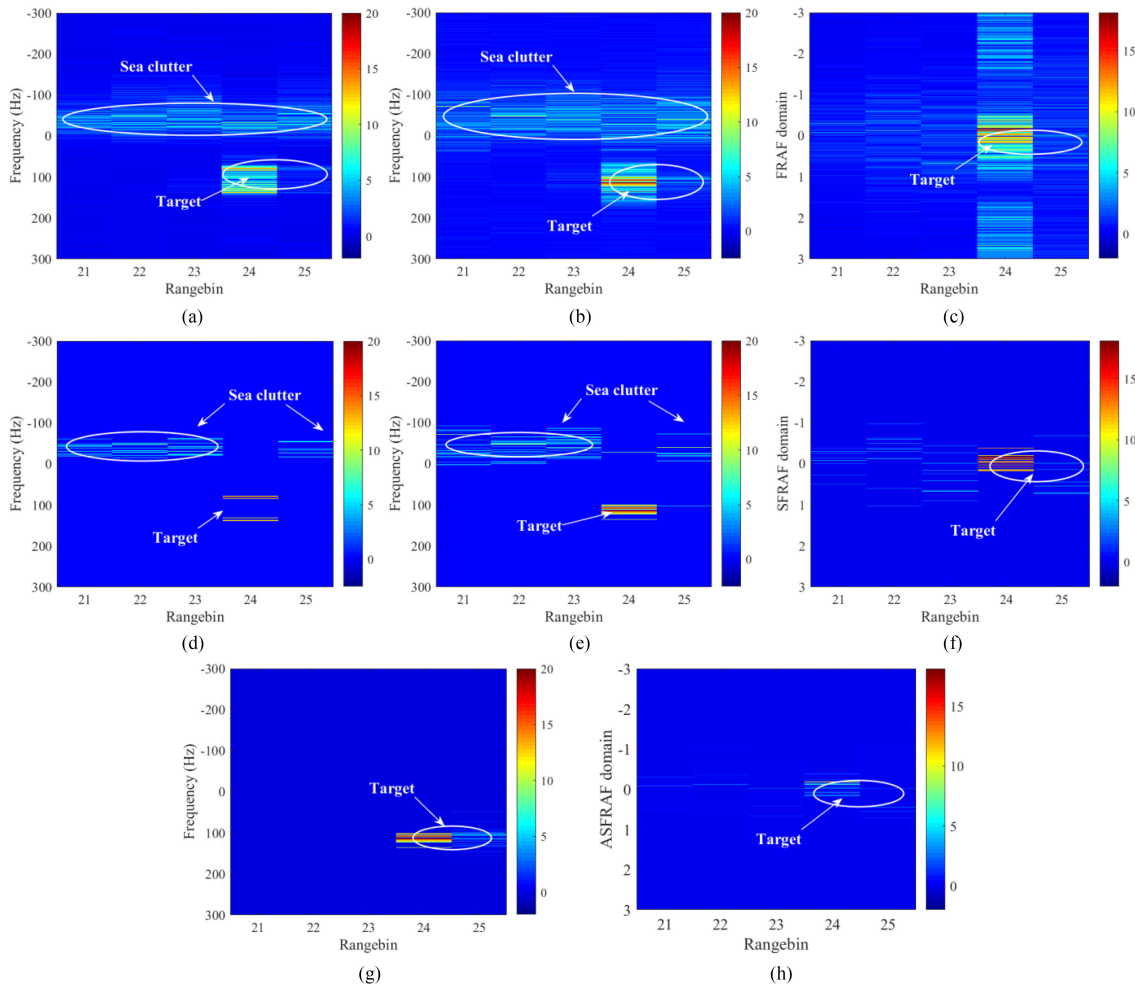


Fig. 11. Range versus Doppler domain detection using different methods (TFC17-006). (a) MTD. (b) FRFT. (c) FRAF. (d) SFT [10]. (e) SFRFT [18]. (f) SFRAF [23]. (g) RSRFT [22]. (h) ASFRAF.

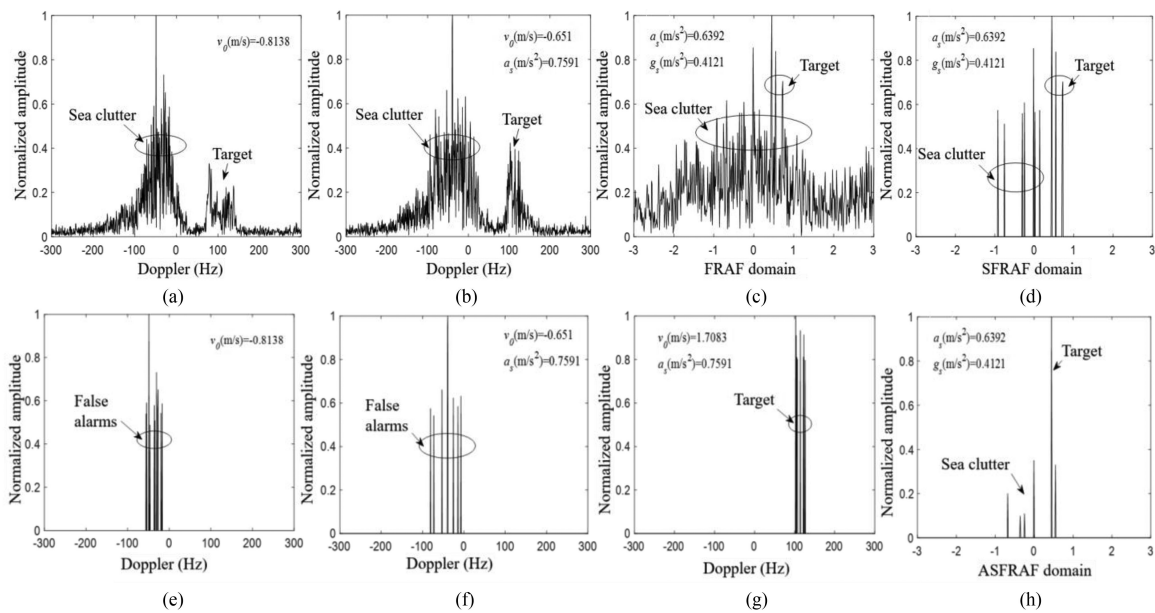


Fig. 12. Target detection using different methods (TFC17-006, Rangebin 25). (a) MTD. (b) FRFT. (c) FRAF. (d) SFRAF [23]. (e) SFT [10]. (f) SFRFT [18]. (g) RSRFT [22]. (h) ASFRAF.

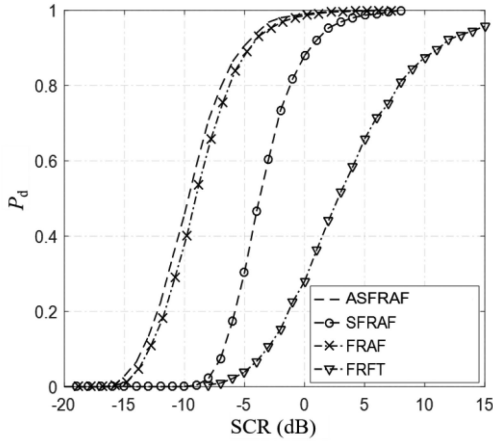


Fig. 13. SCR versus  $P_d$  curves of different detection methods.

It can be seen from the table that after the ASFRF domain processing, the peak difference between the target and the sea clutter is significantly increased, and the sea clutter is greatly suppressed. Taking the sparsity  $K = 7$  as an example, the peak difference increases from 0.0495 of FFT, 0.3682 of FRFT, 0.3224 of FRAF, 0.3682 of SFRFT, 0.3462 of SFRAF to 0.8374 of ASFRF. Due to the iteration of the adaptive filter, calculation time of the proposed method is a more time-consuming compared with SFRAF. However, its computational efficiency is still at least 50% higher than that of the FRAF method. This is due to the SFT and hierarchical iterative kurtosis search method. It should be noted that the calculation time given here is the average time calculated by MATLAB software. If optimized by the program, the proposed algorithm will be more obvious than the FRAF in terms of computational efficiency.

The data of the maneuvering target rangebin are selected for the demonstration of detection performance of ASFRF domain algorithm for real measured data. Fig. 10 shows the time-frequency analysis of the 21#~25# rangebins. The data segments with the starting time  $t_0 = 26$  s, the number of sampling points  $N = 8192$ , and the observation time  $T_n = 1.6384$  s are selected, which are processed by FFT, SFT, FRFT, SFRFT, RSFRFT, FRAF, SFRAF, and ASFRF algorithms, respectively. For the SFT, SFRFT, and SFRAF algorithms, the preset value of the sparsity is  $K = 10$ , and for ASFRF,  $\tau = 2$  ms,  $\chi = 0.97$ ,  $\mu = 1.9$ . It can be found from the figure that the marine target Doppler exhibits time-varying characteristic and high-order motion.

Fig. 11 shows a comparison of the 2-D detection results (rangebin versus Doppler) using different methods. It can be found:

- 1) The FRFT-based method [see Fig. 11(b), (e), (g)] has better energy aggregation of the target signal than the FT-based method [see Fig. 11(a), (d)].
- 2) Since there is no clutter suppression capability, there are many clutter false alarm points in the detection results of the SFT algorithm and SFRFT algorithm, and there are a large number of missing points of the target.
- 3) The RSFRFT algorithm can detect the target well, and there is less clutter false alarms in the rangebin versus Doppler figure.

- 4) The FRAF-based method [see Fig. 11(c), (f)] has better energy aggregation ability for maneuvering targets than the FRFT-based method, but there are still clutter residuals of SFRAF. Using the ASFRF domain adaptive filtering, the sea clutter is better suppressed.

In order to more clearly compare the detection results of different methods, Fig. 12 shows the detection parameter estimation results of the 25th rangebin of TFC17-006 data. In this rangebin, the target spectrum is extremely weak and is subjected to strong clutter interference, making the detection more difficult. It can be seen from the figure that neither the SFT nor the SFRFT algorithm can detect the target. In the SFRAF detection result, the target is influenced by strong clutter interference, which leads to a serious decline in detection performance. It should be noted that due to the characteristics of the adaptive filter itself, the ASFRF domain algorithm cannot completely eliminate the clutter, but it can suppress the sea clutter to the greatest extent while preserving the target's energy, thereby improving the target detection performance in strong clutter backgrounds.

#### D. Detection Performance Analysis

The detection performance of the proposed algorithm is further analyzed by Monte Carlo simulation. The same target's motion parameters and sea clutter data in Table II are used, and the number of sampling points is  $N = 4096$ . The maneuvering target signal is processed by four methods, i.e., FRFT, FRAF, SFRAF, and ASFRF algorithms, where  $K = 5$  and  $B = 128$  of SFRAF,  $\tau = 1.6$  ms,  $\chi = 0.97$ , and  $\mu = 1.9$  of ASFRF. Under the condition of  $P_{fa} = 10^{-3}$ ,  $10^5$  Monte Carlo simulation calculations were performed on different SCRs. Fig. 13 shows the detection performance curves (SCR versus  $P_d$ ) of the four methods. It can be seen from the figure that due to the model mismatch, the detection performance of the FRFT algorithm for the maneuvering target is significantly different from that of the other three methods. Compared with SFRAF, The detection performance of the proposed algorithm is improved by about 6 dB, and it is slightly better than the FRAF algorithm due to the adaptive filtering procedure. Under lower SCR conditions ( $-10$  dB), it still has better detection performance.

## VI. CONCLUSION

In this article, by introducing the adaptive filtering method into SFRAF processing, a novel adaptive clutter suppression and radar maneuvering target detection algorithm named as ASFRF is proposed. The simulations and experiments using real radar data verified the advantages:

- 1) ASFRF algorithm can overcome the influence of the unknown sparsity value and enhance the robustness of SFRAF algorithm, which is more practicable.
- 2) ASFRF algorithm can suppress the clutter effectively while retaining the signal energy to the greatest extent, and has good detection performance for the maneuvering target in low SCR conditions ( $-10$  dB), which is more suitable for clutter background than SFRAF.
- 3) The detection performance of ASFRF algorithm for maneuvering targets with jerk and high-order motions is

as good as FRAF method, which provides a new way for target with complex motion characteristics.

- 4) Due to the iteration process, the calculation time of AS-FRAF is more time-consuming compared with SFRAF. However, due to the utilization of SFT and hierarchical iterative kurtosis search method, the computational efficiency of proposed method is still at least 50% higher than that of the FRAF method.
- 5) The performance of ASFRAF is closely related to the edition of SFT or ADT-SFT, and also some information of the spectrum of the target may be lost in low SCR.

In a word, the proposed adaptive clutter suppression and maneuvering target detection method is not only suitable for maneuvering target with complex motion characteristics in clutter background, but also can meet the requirements for the real-time processing of large-size signals, which provides a practical solution for applications in complex environments. In the future, we will further verify the detection performance of the proposed algorithm in different clutter environments and also study the problem of long-time processing for range and Doppler migrations.

#### ACKNOWLEDGMENT

The authors would like to thank the anonymous reviewers for the valuable comments and suggestions.

#### REFERENCES

- [1] X. L. Chen, J. Guan, X. Y. Li, and Y. He, "Effective coherent integration method for marine target with micromotion via phase differentiation and radon-Lv's distribution," *IET Radar Sonar Navigat.*, vol. 9, no. 9, pp. 1284–1295, 2015.
- [2] L. R. Moyer, J. Spak, and P. Lamanna, "A multi-dimensional hough transform-based track-before-detect technique for detecting weak targets in strong clutter backgrounds," *IEEE Trans. Aerosp. Electron. Syst.*, vol. 47, no. 4, pp. 3062–3068, Nov. 2011.
- [3] X. L. Chen, J. Guan, Z. H. Bao, and Y. He, "Detection and extraction of target with micro-motion in spiky sea clutter via short-time fractional Fourier transform," *IEEE Trans. Geosci. Remote Sens.*, vol. 52, no. 2, pp. 1002–1018, Feb. 2014.
- [4] T. Thayaparan and S. Kennedy, "Detection of a manoeuvring air target in sea-clutter using joint time-frequency analysis techniques," *IEE Proc.—Radar, Sonar Navigat.*, vol. 151, no. 1, pp. 19–30, 2004.
- [5] X. L. Li, Z. Sun, T. S. Yeo, W. Yi, G. L. Cui, and L. J. Kong, "STGRFT for detection of maneuvering weak target with multiple motion models," *IEEE Trans. Signal Process.*, vol. 67, no. 7, pp. 1902–1917, Apr. 2019.
- [6] X. L. Chen, Y. Huang, N. B. Liu, J. Guan, and Y. He, "Radon-fractional ambiguity function-based detection method of low-observable maneuvering target," *IEEE Trans. Aerosp. Electron. Syst.*, vol. 51, no. 2, pp. 815–833, Apr. 2015.
- [7] F. I. Urzaiz, Á. D. de Quevedo, A. M. Ayuso, Á. G. Machado, J. G. Menoyo, and A. A. López, "Design, implementation and first experimental results of an X-band ubiquitous radar system," in *Proc. IEEE Radar Conf.*, Oklahoma City, OK, USA, 2018, pp. 1150–1155.
- [8] B. Friedlander, "Waveform design for MIMO radars," *IEEE Trans. Aerosp. Electron. Syst.*, vol. 43, no. 3, pp. 1227–1238, Jul. 2007.
- [9] X. L. Chen, B. X. Chen, J. Guan, Y. Huang, and Y. He, "Space-range-doppler focus-based low-observable moving target detection using frequency diverse array MIMO radar," *IEEE Access*, vol. 6, pp. 43892–43904, 2018.
- [10] D. Pastina *et al.*, "Maritime moving target long time integration for GNSS-based passive bistatic radar," *IEEE Trans. Aerosp. Electron. Syst.*, vol. 54, no. 6, pp. 3060–3083, Dec. 2018.
- [11] G. Wang, X.-G. Xia, B. T. Root, V. C. Chen, Y. Zhang, and M. Amin, "Manoeuvring target detection in over-the-horizon radar using adaptive clutter rejection and adaptive chirplet transform," *IEE Proc.—Radar, Sonar Navigat.*, vol. 150, no. 4, pp. 292, Aug. 2003.
- [12] Z. Sun, X. L. Li, W. Yi, G. L. Cui, and L. J. Kong, "Detection of weak maneuvering target based on keystone transform and matched filtering process," *Signal Process.*, vol. 140, pp. 127–138, Nov. 2017.
- [13] X. L. Chen, J. Guan, Y. He, and X. H. Yu, "High-resolution sparse representation and its applications in moving target detection," *J. Radars*, vol. 6, no. 3, pp. 239–251, 2017.
- [14] A. Karine, A. Toumi, A. Khenchaf, and M. El Hassouni, "Target recognition in radar images using weighted statistical dictionary-based sparse representation," *IEEE Geosci. Remote Sens. Lett.*, vol. 14, no. 12, pp. 2403–2407, Dec. 2017.
- [15] Z. Zhang, Y. Xu, J. Yang, X. Li, and D. Zhang, "A survey of sparse representation: algorithms and applications," *IEEE Access*, vol. 3, pp. 490–530, 2015.
- [16] X. L. Chen, J. Guan, Y. L. Dong, and Y. He, "Sea clutter suppression and micromotion target detection in sparse domain," *Acta Electronica Sinica*, vol. 44, no. 4, pp. 860–876, 2016.
- [17] Z. Zhao, R. Tao, G. Li, and Y. Wang, "Sparse fractional energy distribution and its application to radar detection of marine targets with micro-motion," *IEEE Sensors J.*, vol. 19, no. 24, pp. 12165–12174, Dec. 2019.
- [18] H. Hassanieh, P. Indyk, D. Katabi, and E. Price, "Simple and practical algorithm for sparse Fourier transform," in *Proc. 23rd Annu. ACM-SIAM Symp. Discrete Algorithms*, Kyoto, Japan, Jan. 2012, pp. 1183–1194.
- [19] H. Hassanieh, P. Indyk, D. Katabi, and E. Price, "Nearly optimal sparse Fourier transform," in *Proc. 44th Annu. ACM Symp. Theory Comput.*, NY, USA, May 2012, pp. 563–578.
- [20] S. Wang, V. M. Patel, and A. Petropulu, "Multidimensional sparse Fourier transform based on the Fourier projection-slice theorem," *IEEE Trans. Signal Process.*, vol. 67, no. 1, pp. 54–69, Jan. 2019.
- [21] A. López-Parrado and J. Velasco-Medina, "Cooperative wideband spectrum sensing based on sub-Nyquist sparse fast Fourier transform," *IEEE Trans. Circuits Syst. II, Express Briefs*, vol. 63, no. 1, pp. 39–43, Jan. 2016.
- [22] S. Pawar and K. Ramchandran, "FFAST: An algorithm for computing an exactly  $k$ -Sparse DFT in  $O(k \log k)$  time," *IEEE Trans. Inf. Theory*, vol. 64, no. 1, pp. 429–450, Jan. 2018.
- [23] S. H. Liu *et al.*, "Sparse discrete fractional Fourier transform and its applications," *IEEE Trans. Signal Process.*, vol. 62, no. 24, pp. 6582–6595, Dec. 2014.
- [24] G. Chen, S. Tsai, and K. Yang, "On performance of sparse fast Fourier transform and enhancement algorithm," *IEEE Trans. Signal Process.*, vol. 65, no. 21, pp. 5716–5729, Nov. 2017.
- [25] S. Wang, V. M. Patel, and A. Petropulu, "The robust sparse Fourier transform (RSFT) and its application in radar signal processing," *IEEE Trans. Aerosp. Electron. Syst.*, vol. 53, no. 6, pp. 2735–2755, Dec. 2017.
- [26] X. H. Yu, X. L. Chen, Y. Huang, L. Zhang, J. Guan, and Y. He, "Radar moving target detection in clutter background via adaptive dual-threshold sparse Fourier transform," *IEEE Access*, vol. 7, no. 99, pp. 58200–58211, May 2019.
- [27] X. H. Yu, X. L. Chen, Y. Huang, and J. Guan, "Fast detection method for low-observable maneuvering target via robust sparse fractional Fourier transform," *IEEE Geosci. Remote Sens. Lett.*, pp. 1–5, 2019, doi: 10.1109/LGRS.2019.2939264.
- [28] X. H. Yu, X. L. Chen, J. Guan, and Y. Huang, "Radar marine maneuvering target detection via high resolution sparse fractional ambiguity function," *J. Commun.*, vol. 40, no. 8, pp. 72–84, 2019.
- [29] S. Dixit and D. Nagaria, "LMS adaptive filters for noise cancellation: A review," *Int. J. Elect. Comput. Eng.*, vol. 7, no. 5, pp. 2520–2529, Oct. 2017.
- [30] Z. F. Li, D. Li, X. L. Xu, and J. Q. Zhang, "New normalized LMS adaptive filter with a variable regularization factor," *J. Syst. Eng. Electron.*, vol. 30, no. 2, pp. 259–269, Apr. 2019.
- [31] M. V. Matsuo, E. V. Kuhn, and R. Seara, "Stochastic analysis of the NLMS algorithm for nonstationary environment and deficient length adaptive filter," *Signal Process.*, vol. 160, pp. 190–201, 2019.
- [32] D. I. Kim and P. D. Wild, "Performance analysis of the DCT-LMS adaptive filtering algorithm," *Signal Process.*, vol. 80, pp. 1629–1654, 2010.
- [33] M. I. Doroslovacki and H. Fan, "Wavelet-based linear system modeling and adaptive filtering," *IEEE Trans. Signal Process.*, vol. 44, no. 5, pp. 1156–1167, May 1996.
- [34] S. Attallah, "The wavelet transform-domain LMS algorithm: A more practical approach," *IEEE Trans. Circuits Syst. II, Analog Digit. Signal Process.*, vol. 47, no. 3, pp. 209–213, Mar. 2000.
- [35] J. Guan, X. L. Chen, Y. Huang, and Y. He, "Adaptive fractional Fourier transform-based detection algorithm for moving target in heavy sea clutter," *IET Radar Sonar Navigat.*, vol. 6, no. 5, pp. 389–401, 2012.

- [36] H. J. de Wind, J. C. Cilliers, and P. L. Herselman, "DataWare: Sea clutter and small boat radar reflectivity databases," *IEEE Signal Process. Mag.*, vol. 27, no. 2, pp. 145–148, Mar. 2010.
- [37] L. K. Ting, C. F. N. Cowan, R. F. Woods, and P. R. Cork, "Tracking performance of leakage LMS for chirped signal," in *Proc. IEEE Workshop Signal Process. Syst.*, 2001, pp. 101–108.



**Xiaolong Chen** was born in Yantai, Shandong, China, in 1985. He received the master's degree in signal and information processing in 2010, and the Ph.D. degree in information and communication engineering in 2014, all from Naval Aviation University (NAU), Shandong.

From 2015 to 2017, he was a Lecturer with Marine Target Detection Research Group, NAU, where he lectures "Radar Principle." He is currently an Associate Professor with NAU. He has published more than 80 academic articles, two books, and holds 36

national invention patents. His current research interests include radar signal processing especially for marine target detection, moving target detection, micro-Doppler, and clutter suppression. He has given more than 20 speeches of radar signal processing especially marine target.

Dr. Chen was selected in the Young Talents Program of China Association for Science and Technology (CAST), in 2016 and received the Excellent Doctor Dissertation of CIE. In 2017, he received the Chinese Patent Award. He received four excellent papers awards at 2016 International Radar Conference, 2017 EAI International Conference on Machine Learning and Intelligent Communications, the 14th National Radar Conference, and 2019 IEEE 2nd International Conference on Electronic Information and Communication Technology (ICEICT 2019), respectively. In 2017 and 2018, his papers were selected as highly cited paper of Journal of Radars, and F5000 Top Articles from Outstanding S&T Journals of China. In 2019, he received the Civil-Military Integration Award of China Industry-University-Research Institute Collaboration Association. He was selected for the Young Scientist Award both at 2019 URSI Asia-Pacific Radio Science Conference and 2019 International Applied Computational Electromagnetics Society Symposium, China. He is the senior member of CIE and has served as the Committee Member of CIE Youth Commission, and Vice Executive Secretary of Radar and Information System Committee of CIE Young Scientist Club since 2018. He was the TPC member of the 2015 and 2018 IET International Radar Conference. He was the Section Chair of 2016 International Conference on Mathematical Characterization, Analysis and Applications of Complex Information, 2017 MLICOM, 2017 International Conference on Radar Systems (UK), 2019 ICEICT, and 2019 ACES. He is an Organizer of the special session "Recent Development on Radar Signal Processing" of 2019 ICEICT, special session "Radar Marine Target Detection and Recognition" of ACES 2019, and workshop "Advances in Radar Signal Processing and Target Recognition" of International Conferences on Communications Signal Processing and Systems (CSPS 2019). He has been in the Editorial Board of *Journal of Radars* since 2019 and served as an Associate Editor of IEEE ACCESS since 2018. He is a Reviewer for IEEE TSP, IEEE SPL, IEEE TGRS, IEEE GRSL, IEEE JSTARS, IET RSN, IET SP, IET EL, DSP, and many international conferences.



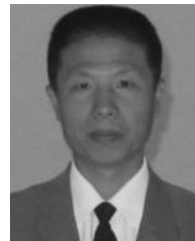
**Xiaohan Yu** was born in Hebei, China, in 1991. She received the M.S. and Ph.D. degrees in information and communication engineering from Naval Aviation University, Shandong, China, in 2015 and 2019, respectively.

She is currently an Engineer with Naval Research Academy. Her main research interests include radar moving target detection and sparse signal processing.



**Yong Huang** was born in Hunan, China, in 1979. He received the M.S. and Ph.D. degree in information and communication engineering from Naval Aviation University (NAU), Shandong, China, in 2005 and 2010, respectively.

From 2011 to 2016, he has been a Lecturer with the Department of Electronic and Information Engineering, NAU. He is also an Associate Professor with NAU. His current research interests include radar signal processing and clutter rejection.



**Jian Guan** received the Ph.D. degree in electronic engineering from Tsinghua University, Beijing, China, in 2000.

He is currently a Professor with Naval Aviation University. His research interests include radar target detection and tracking, image processing, and information fusion. He has authored numerous papers in his areas of expertise and holds 21 national invention patents. He is the author of two books related to radar detection. He is in the Editorial Boards of many radar related journals. He has served in the technical

committee of many international conferences on radar.

Dr. Guan is a Senior Member of the CIE and committee member of Radio Positioning Technology Branch in CIE. He has won the prize of the National Excellent Doctoral Dissertation, "Realistic Outstanding Youth Practical Engineering Award" of CAST, and was selected for National Talents Engineering of Ministry of Personnel of China.